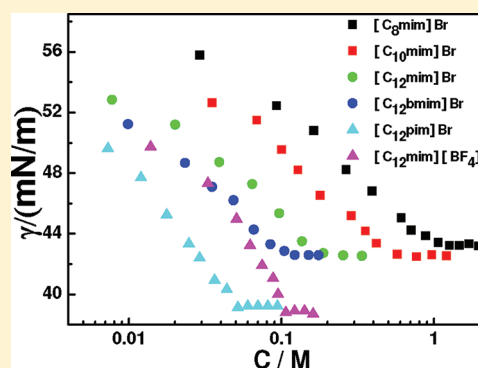


# Aggregation Behavior of Surface Active Imidazolium Ionic Liquids in Ethylammonium Nitrate: Effect of Alkyl Chain Length, Cations, and Counterions

Lijuan Shi and Liqiang Zheng\*

Key Laboratory of Colloid and Interface Chemistry, Shandong University, Ministry of Education, Jinan 250100, China

**ABSTRACT:** The aggregation behavior of surface active imidazolium ionic liquids (ILs) with different alkyl chain length, cations, and counterions, namely, 1-alkyl-3-methylimidazolium bromide ( $[C_n\text{mim}]\text{Br}$  ( $n = 8, 10, 12$ )), 1-dodecyl-2,3-dimethylimidazolium bromide ( $[C_{12}\text{bmim}]\text{Br}$ ), 1-(2,4,6-trimethylphenyl)-3-dodecylimidazolium bromide ( $[C_{12}\text{pim}]\text{Br}$ ), and 1-dodecyl-3-methylimidazolium tetrafluoroborate ( $[C_{12}\text{mim}][\text{BF}_4]$ ) in a protic room temperature IL, ethylammonium nitrate (EAN), was investigated through surface tension measurements and  $^1\text{H}$  NMR spectroscopy. Surface tension results show that surface properties and micellization behavior of surface active ILs in EAN are significantly affected by the structure of the cations, the basicity of counterions, and the hydrophobicity of alkyl chains. A detailed analysis of chemical shifts of various protons of surface active ILs and EAN was employed to investigate the micelle formation mechanism. Hydrogen bonding interaction is found to occur between the protons at C-2 on the imidazolium ring and the oxygen atoms in  $[\text{NO}_3]^-$  anions, and the interaction varies as a function of the basicity of the counterions and the hydrophobicity of the side-chains bonded to the imidazolium ring. The micelle formation may be accompanied by a partial changeover from trans to gauche conformations in the alkyl chain. The solvophobic effect may exist between the hydrophobic portion of  $[\text{CH}_3\text{CH}_2\text{NH}_3]^+$  and the hydrophobic chains of the surface active ILs.



## 1. INTRODUCTION

Ionic liquids (ILs) are receiving much attention due to their special properties, such as low volatility, nonflammability, high thermal stability, high ionic conductivity, and easy recyclability.<sup>1,2</sup> Their physicochemical properties can be easily modulated by suitable selection of cations and anions. An interesting characteristic of ILs is that the cations, such as 1-alkyl-3-methylimidazolium ( $[C_n\text{mim}]^+$ ), possess an inherent amphiphilicity.<sup>3</sup> Therefore, these ILs could exhibit as novel surfactants, thereby self-assembling to form aggregates with specific structure, shape, and properties. Due to the possibility of fine-tuning amphiphilicity of ILs by changing the alkyl chain length, the type of cations, and the nature of the counterions, one can change the structures of these aggregates.

Recently, a large amount of research has focused on the effect of alkyl chain length, the cations and the counterions on the aggregation behavior of ILs in aqueous solution.<sup>3–12</sup> Bowers et al. first reported the aggregation behavior of 1-butyl-3-methylimidazolium tetrafluoroborate ( $[C_4\text{mim}][\text{BF}_4]$ ), 1-octyl-3-methylimidazolium chloride ( $[C_8\text{mim}]\text{Cl}$ ), and 1-octyl-3-methylimidazolium iodide ( $[C_8\text{mim}]\text{I}$ ) in aqueous solution and established the role of the alkyl chain length and counterions on the aggregation behavior of these ILs.<sup>3</sup> Goodchild et al. explored the aggregation behavior of 1-alkyl-3-methylimidazolium bromide ( $[C_n\text{mim}]\text{Br}$ ,  $n = 2–10$ ) in water, where the critical micelle concentrations (CMCs) for  $[C_n\text{mim}]\text{Br}$  with  $n > 6$  were detected.<sup>4</sup> Then the role of the alkyl chain length and the counterions on the aggregation behavior of the  $[C_n\text{mim}]\text{X}$

( $X = \text{Cl}$ ,  $[\text{PF}_6]$ , or  $[\text{NTf}_2]$ ) family was systematically investigated by Rebelo and Lopes et al.,<sup>5</sup> who observed that only  $[C_n\text{mim}]\text{Cl}$  with  $n > 8$  unambiguously form aggregates in solution and no micelle formation was detected when the  $\text{Cl}^-$  anion in  $[C_{10}\text{mim}]\text{Cl}$  was replaced by  $[\text{NTf}_2]^-$  or  $[\text{PF}_6]^-$ . As a continuation of research, they also observed that the cationic ring types have a significant effect on the CMC values of the surface active ILs, 1-dodecyl-3-methylpyridinium bromide ( $[C_{12}\text{mpy}]\text{Br}$ ), 1-methyl-1-dodecylpiperidinium bromide ( $[C_{12}\text{mpip}]\text{Br}$ ), and 1-methyl-1-dodecylpyrrolidinium ( $[C_{12}\text{mpyr}]\text{Br}$ ) in aqueous solution.<sup>6</sup> Then Wang et al. deduced that the hydrophobicity and steric hindrance of the cations play important roles in the aggregation behavior of  $[C_8\text{mim}]\text{Br}$ , 1-octyl-4-methylpyridinium bromide (4 m- $[C_8\text{pyr}]\text{Br}$ ), and  $[C_8\text{mpyr}]\text{Br}$ .<sup>7</sup> They also reported that the anionic effect basically follows the Hofmeister series, and the ability of anionic hydration is predominant for the aggregation behavior of the 1-octyl-3-methylimidazolium ILs.<sup>7</sup> The nature of the effect of alkyl chain length, the cations and the counterions on the aggregation behavior have also been investigated. Headley et al. have verified through  $^1\text{H}$  NMR that imidazolium ILs can form intermolecular hydrogen bonding with water, and there is a competition for the hydrogen bonding with the aromatic hydrogens for the solvent molecules and the counterions.<sup>8,9</sup> The structures of aggregates formed by the ILs,  $[C_4\text{mim}][\text{Cl}]$ ,

Received: November 24, 2011

Revised: January 22, 2012

Published: January 23, 2012

$[\text{C}_8\text{mim}][\text{Cl}]$ ,  $[\text{C}_4\text{mim}][\text{BF}_4]$ , and  $[\text{C}_4\text{mpy}][\text{Cl}]$ , in aqueous solution were determined through  $^1\text{H}$  NMR by Singh et al.,<sup>10</sup> who found that aggregation-induced conformational changes depend on the aromatic ring, alkyl chain, counterions, and their interactions with water.

Due to their special properties, room-temperature ionic liquids (RTILs) are also receiving significant attention as novel solvents to support surfactant self-assembly.<sup>13</sup> There are two kinds of RTILs which are relevant for their use in self-assembly, that is, the protic ionic liquids (PILs) and aprotic ionic liquids (AILs). The PILs, such as ethylammonium nitrate (EAN), have the potential to form a three-dimensional hydrogen bonding network, which is beneficial to the surfactant self-assembly.<sup>14</sup> The aggregation behaviors of alkyltrimethylammonium bromide, alkylpyridinium bromide, and nonionic Triton X-100 in EAN were first reported by Evans et al.<sup>15,16</sup> It was found that the CMC values are about five to ten times larger than those obtained in water. Velasco et al. investigated the aggregation behavior of alkylammonium nitrate amphiphiles in EAN and observed that the formation of micelles did not cause a change in the partial molar volume of EAN, which is in contrast to the case in water.<sup>17</sup> Structures of micelles formed by polyoxyethylene alkyl ether nonionic surfactants,  $\text{C}_n\text{E}_m$ , in EAN were reported by Warr et al.<sup>18</sup> The micelle structures change systematically with alkyl and ethoxy chain length, in parallel with observations in aqueous solution. More recently, research has focused on the aggregation behavior of surface active ILs in RTILs, including EAN.<sup>19–21</sup> This kind of pure IL system may have potential applications with some advantages, such as high thermal stability and fine-tuning properties.<sup>19</sup> Kunz et al. reported the aggregation of  $[\text{C}_{16}\text{mim}]\text{Cl}$  and  $[\text{C}_{16}\text{mim}][\text{BF}_4]$  in ethylammonium nitrate (EAN) and observed that the CMC for  $[\text{C}_{16}\text{mim}][\text{BF}_4]$  is lower than  $[\text{C}_{16}\text{mim}]\text{Cl}$ .<sup>19</sup> Then our group investigated the aggregation behavior of  $[\text{C}_n\text{mim}]\text{Br}$  ( $n = 12, 14, 16$ ) in EAN by surface tension measurements at various temperatures.<sup>20</sup> However, few studies have focused on the formation mechanism and structures of aggregates formed by surface active ILs in RTILs. The intermolecular interactions

among the cations, counterions, and solvent molecules during micellization are still unclear.

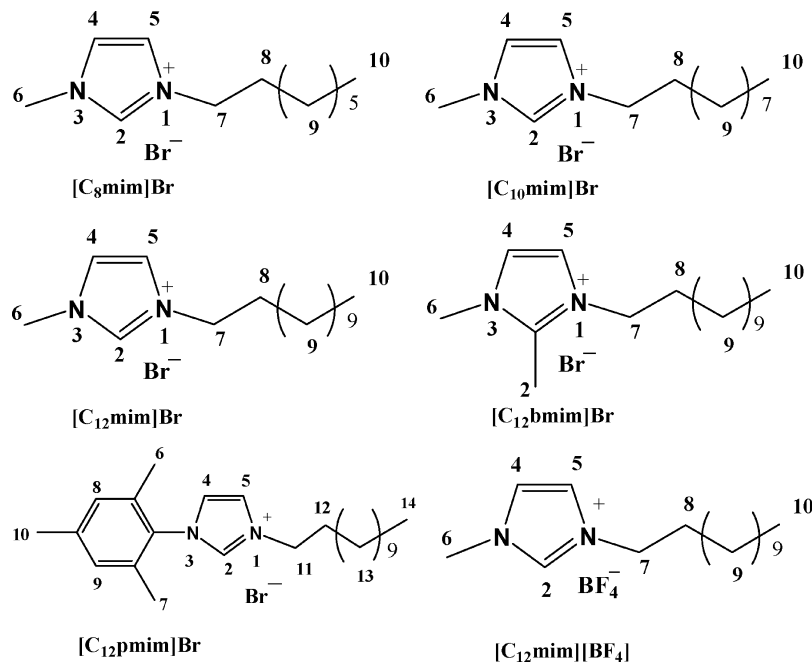
In the present work, we prepared a series of ILs with different alkyl chain length, cations, and counterions, that is,  $[\text{C}_n\text{mim}]\text{Br}$  ( $n = 8, 10, 12$ ),  $[\text{C}_{12}\text{mim}][\text{BF}_4]$ , 1-dodecyl-2,3-dimethylimidazolium bromide ( $[\text{C}_{12}\text{bmim}]\text{Br}$ ), as well as 1-(2,4,6-trimethylphenyl)-3-dodecylimidazolium bromide ( $[\text{C}_{12}\text{pim}]\text{Br}$ ) (see Scheme 1 for their chemical structures). The aggregation behaviors of these ILs in EAN have been investigated by surface tension measurement and  $^1\text{H}$  NMR spectroscopy. Our aim is to establish the dependence of the aggregation of the surface active ILs on the cations, counterions, and alkyl chain length and thus to offer a systematic study in the formation mechanism of aggregates formed by surface active ILs in RTILs.

## 2. EXPERIMENTAL SECTION

**2.1. Materials.** 1-Methylimidazole (98%), 1,2-dimethylimidazole (98%),  $\text{CDCl}_3$  (99.96%), and  $\text{D}_2\text{O}$  (99.96%) were purchased from Sigma-Aldrich. 1-bromooctane (97%), 1-bromodecane (97%), 1-bromododecane (97%), 2,4,6-trimethylaniline (98%) and lithium tetrafluoroborate (99.9%) were purchased from Aladdin Reagent Company. Ethylamine (65–70%), nitric acid (65%), phosphoric acid (85%), formaldehyde (37%), ammonium chloride, glyoxal, ethyl acetate, acetonitrile, tetrahydrofuran, toluene, and diethyl ether were the products of Beijing Chemical Reagent Company. All the ILs used in this study were synthesized in our laboratory, and the purity of the products were ascertained by  $^1\text{H}$  NMR spectra in  $\text{CDCl}_3$ .

**2.2. Synthesis of  $[\text{C}_n\text{mim}]\text{Br}$  ( $n = 8, 10$ ).** For the synthesis of  $[\text{C}_8\text{mim}]\text{Br}$ , 1-methylimidazole (0.1 mol) and 1-bromooctane (0.12 mol) were mixed in ethyl acetate and the mixture was refluxed under nitrogen atmosphere for 24 h. After being cooled to room temperature, the biphasic system was separated to give the product as viscous liquid. Then the resulting product was washed with ethyl acetate at least three times. After removal of ethyl acetate by evaporation under reduced pressure, the product was dried in vacuo at  $50^\circ\text{C}$  to obtain a colorless

Scheme 1. Chemical Structures of the Surface Active Imidazolium ILs Used in This Study



liquid.<sup>22</sup> The  $[C_{10}mim]Br$  was synthesized following the synthetic procedure for  $[C_8mim]Br$ .

**2.3. Synthesis of  $[C_{12}mim]Br$ .** 1-Methylimidazole (0.1 mol) and 1-bromododecane (0.12 mol) were dissolved in acetonitrile, and the mixture was stirred at 75–80 °C under nitrogen atmosphere for 48 h. The solvent was removed by evaporation under reduced pressure. The product was purified by recrystallization from ethyl acetate at least four times and then dried in vacuo for 48 h.<sup>23</sup>

**2.4. Synthesis of  $[C_{12}pim]Br$ .** For the synthesis of  $[C_{12}pim]Br$ , the (2, 4, 6-trimethylphenyl)imidazole was first synthesized following the procedure reported previously.<sup>24</sup> A mixture of aqueous glyoxal (0.1 mol) and 2,4,6-trimethylaniline (0.1 mol) in methanol was stirred at room temperature until a yellow precipitate formed. After addition of ammonium chloride (0.2 mol), formaldehyde solution (37%, 0.21 mol), and phosphoric acid (85%, 14 mL), the solution was refluxed for 9 h. The majority of the solvent (ca. 85%) was removed in vacuo, and then the pH value of the solution was adjusted to 9 with KOH. The product was extracted with dichloromethane and then the solvent was removed in vacuo. The final product was purified by recrystallization using tetrahydrofuran at least four times. For the synthesis of  $[C_{12}pim]Br$ , (2,4,6-trimethylphenyl)imidazole (0.1 mol) and 1-bromododecane (0.12 mol) were mixed in dry toluene and the mixture was refluxed at 110 °C under nitrogen atmosphere for 48 h. The obtained product was cooled to room temperature and purified by recrystallization in diethyl ether at least four times. The final product was dried in vacuo for 48 h.

**2.5. Synthesis of  $[C_{12}bmim]Br$ .** 1,2-Dimethylimidazole (0.1 mol) and 1-bromododecane (0.12 mol) were dissolved in acetonitrile, and the mixture was stirred at 60 °C under nitrogen atmosphere for 3 days. The solvent was removed by evaporation under reduced pressure. The product was purified by recrystallization from ethyl acetate at least four times and then dried in vacuo for 48 h.<sup>25</sup>

**2.6. Synthesis of  $[C_{12}mim][BF_4]$ .** 1-Dodecyl-3-methylimidazolium tetrafluoroborate was synthesized following the procedure of Holbrey et al.<sup>26</sup> A aqueous solution of  $LiBF_4$  was added slowly to a cooled, rapidly stirred aqueous solution of 1-dodecyl-3-methylimidazolium bromide. The product precipitated as a waxy white solid and was collected by filtration. The obtained salt was dissolved in dichloromethane and washed three times with water. Then the solvent was removed by evaporation under reduced pressure to yield the tetrafluoroborate salt. The product was purified by recrystallization in methanol as a colorless crystalline solid, and then dried in vacuo for one week at 50 °C.

**2.7. Synthesis of EAN.** EAN was freshly prepared according to the procedures reported previously.<sup>27</sup> In a typical synthesis, ethylamine (65–70%, 83 mL) was slowly added to nitric acid (65%, 50 mL) under stirring and cooling in an ice bath. Then water in the resulting mixture was removed with a rotary evaporator.

**2.8. Apparatus and Procedures.** Surface tension measurements were carried out on a model JYW-200B tensiometer (Chengde Dahua Instrument Co., Ltd., accuracy  $\pm 0.1$  mN/m) using the ring method. The temperature was controlled at  $25 \pm 0.1$  °C using a thermostatic bath. All measurements were repeated until the values were reproducible.  $^1H$  NMR spectra were run on a Bruker Advance 400 spectrometer equipped with a pulse field gradient module (Z axis) using a 5 mm BBO probe. The instrument was operated at a frequency of 400.13 MHz at  $25 \pm 0.1$  °C. The observed chemical shifts ( $\delta_{obs}$ ) of the discrete protons were examined as a function of concentration below

and above CMC.  $D_2O$  was used as an external chemical shift reference in the coaxial tube.

### 3. RESULTS AND DISCUSSION

#### 3.1. Surface Properties and Micellization Parameters.

Surface tension measurements were performed to investigate the surface activities and micellization behavior of the surface active imidazolium ILs in EAN. Figure 1a–c shows the surface

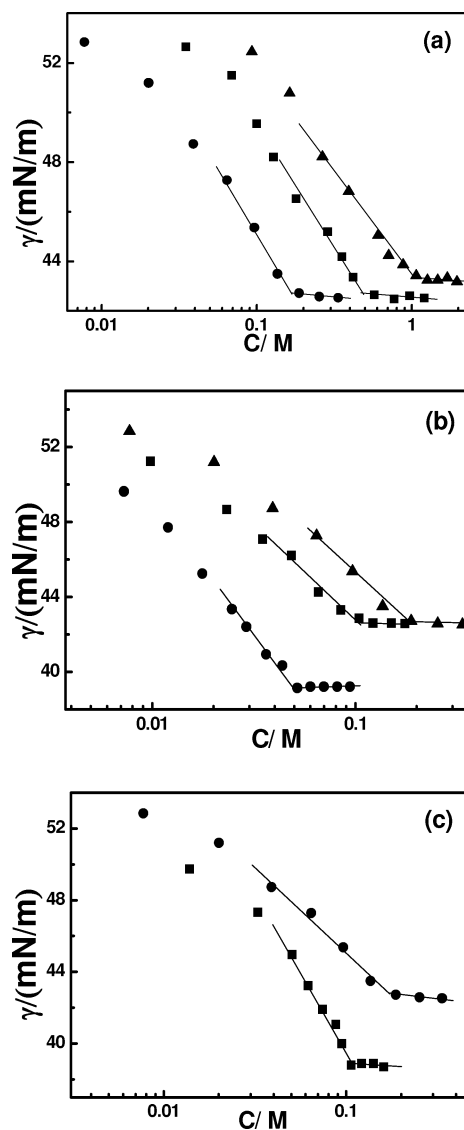


**Figure 1.** Surface tension as a function of concentration for (a)  $[C_8mim]Br$  (▲),  $[C_{10}mim]Br$  (■), and  $[C_{12}mim]Br$  (●); (b)  $[C_{12}bmim]Br$  (■),  $[C_{12}pim]Br$  (●), and  $[C_{12}mim]Br$  (▲); and (c)  $[C_{12}mim][BF_4]$  (■) and  $[C_{12}mim]Br$  (●) in EAN at 25 °C.

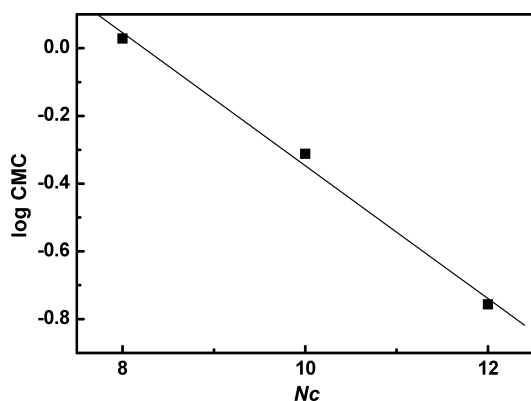
tension ( $\gamma$ ) versus concentration ( $C$ ) plots for ILs with different structures according to Scheme 1 at 25 °C. It is clear that in each ( $\gamma$ – $C$ ) plot, the surface tension decreases initially with increasing concentration and then a distinct break point appears, indicating the formation of micelles. The critical micelle concentration (CMC) was determined from the break point of the plot. The obtained CMC and  $\gamma_{CMC}$  (surface tension at CMC) values for these ILs are listed in Table 1.

Figure 1a shows the ( $\gamma$ – $C$ ) plots for the ILs with different alkyl chain length, that is,  $[C_nmim]Br$  ( $n = 8, 10, 12$ ), in EAN at

**Table 1.** Surface Properties and Micellization Parameters of Different ILs in EAN at 25 °C

ILs	CMC (M)		$\gamma_{\text{CMC}}$ (mN/m)	$\Gamma_{\text{max}}$ ( $\mu\text{mol}/\text{m}^2$ )	$A_{\text{min}}$ ( $\text{\AA}^2$ )
	determined from surface tension	determined from $^1\text{H}$ NMR			
$[\text{C}_8\text{mim}]\text{Br}$	1.068	1.142	43.4	1.59	103.6
$[\text{C}_{10}\text{mim}]\text{Br}$	0.487	0.493	42.5	1.83	90.7
$[\text{C}_{12}\text{mim}]\text{Br}$	0.175	0.181	43.4	2.34	71.0
$[\text{C}_{12}\text{bmim}]\text{Br}$	0.112	0.131	42.6	2.03	81.8
$[\text{C}_{12}\text{pim}]\text{Br}$	0.051	0.048	39.0	2.61	63.6
$[\text{C}_{12}\text{mim}][\text{BF}_4]$	0.107	0.108	38.8	3.66	45.0

25 °C. It can be seen that the CMC values decrease in the order  $[\text{C}_8\text{mim}]\text{Br} > [\text{C}_{10}\text{mim}]\text{Br} > [\text{C}_{12}\text{mim}]\text{Br}$ , along with the increase of hydrophobicity due to the increased length of the hydrocarbon chain. This result indicates that solvophobic interactions exist between the hydrocarbon chain of the  $[\text{C}_n\text{mim}]\text{Br}$  and EAN, similar to the hydrophobic interactions in water. However, compared with the result in aqueous solution,<sup>28,29</sup> the present system exhibits much higher CMC values. This observation is in keeping with the observation of Evans et al.,<sup>15</sup> who believes that EAN is a slightly better solvent than water for hydrocarbons. It is mentioned that no micelle formation was detected when the hydrophobic chain length is shorter than eight, indicating that solvophobic effect plays an important role in micelle formation in EAN. Figure 2 shows the correlation

**Figure 2.** Logarithm of CMC (M) as a function of the number of carbon atoms in hydrophobic chains for  $[\text{C}_n\text{mim}]\text{Br}$  at 25 °C.

between CMC and the number of carbon atoms in the hydrocarbon chain ( $N_c$ ) of  $[\text{C}_n\text{mim}]\text{Br}$ . It can be seen that the logarithm of CMC decreases linearly with the increase of  $N_c$ , following the empirical Stauff-Klevens rule below:<sup>30</sup>

$$\log \text{CMC} = A - BN_c \quad (1)$$

where  $A$  and  $B$  are empirical constants. The value of  $A$  reflects the contribution of the polar head to micelle formation, and  $B$  displays the average contribution of each methylene to the micelle formation. A smaller value of  $A$  or a larger value of  $B$  implies that micelle formation is more favorable.<sup>31</sup> The values of  $A$  and  $B$  for  $[\text{C}_n\text{mim}]\text{Br}$  in EAN obtained from Figure 2 are 1.60 and 0.20, respectively, which are different from those in water ( $A = 1.95$ ,  $B = 0.32$ ).<sup>29</sup> The value of  $B$  is much smaller than that in water, further verifying the weaker solvophobic effect in EAN.

The structures of cations also have significant effect on micellization in EAN. The CMC values for  $[\text{C}_{12}\text{pim}]\text{Br}$  and

$[\text{C}_{12}\text{bmim}]\text{Br}$  are both lower than that of  $[\text{C}_{12}\text{mim}]\text{Br}$ . Generally, the underlying influence of cations on micellization is very complex because head groups have opposing tendencies to keep close to minimize hydrocarbon-solvent contacts and to repel as a result of electrostatic repulsion, solvation, and steric hindrance.<sup>6</sup> When  $[\text{C}_{12}\text{mim}]\text{Br}$  is dissolved in EAN,  $[\text{C}_{12}\text{mim}]^+$  could interact with  $[\text{NO}_3]^-$  through electrostatic interactions. In addition, the proton on C-2 in the  $[\text{C}_{12}\text{mim}]^+$  cation could also form hydrogen bonding with  $[\text{NO}_3]^-$  due to its highly acidic property.<sup>8,32</sup> For  $[\text{C}_{12}\text{mim}]\text{Br}$ , the solvation effect of the headgroup is mainly caused by the electrostatic and the hydrogen bonding interactions with  $[\text{NO}_3]^-$ . By replacing H on C-2 with  $\text{CH}_3$ , the hydrogen bonding interaction between the aromatic ring and  $[\text{NO}_3]^-$  is significantly weakened. Thus, the solvation interaction between the headgroup of  $[\text{C}_{12}\text{bmim}]\text{Br}$  and EAN is much weaker than that between  $[\text{C}_{12}\text{mim}]\text{Br}$  and EAN. That is, the solvophobicity of the headgroup of  $[\text{C}_{12}\text{bmim}]\text{Br}$  is enhanced compared with that of  $[\text{C}_{12}\text{mim}]\text{Br}$ . In addition, the extra nonpolar methyl substituent on C-2 instead of the partially charged H can also enhance the solvophobicity of headgroup.<sup>33</sup> The expected slightly higher solvophobicity of the headgroup of  $[\text{C}_{12}\text{bmim}]\text{Br}$  is probably the reason for the lower CMC value for  $[\text{C}_{12}\text{bmim}]\text{Br}$  than that for  $[\text{C}_{12}\text{mim}]\text{Br}$ . In the case of  $[\text{C}_{12}\text{pim}]\text{Br}$ , two effects compensate each other. On one hand, the incorporation of 2,4,6-trimethylphenyl group enhances the steric hindrance of head groups, which would lead to a higher CMC value in comparison with  $[\text{C}_{12}\text{mim}]\text{Br}$ . On the other hand, the incorporated aryl group makes the charge of headgroup more delocalized, and thus reduces the electrostatic repulsion between head groups. In addition, the solvophobicity of  $[\text{C}_{12}\text{pim}]^+$  is also enhanced due to the incorporation of the aryl group.<sup>34</sup> The two factors above can minimize the adverse effect of steric hindrance on micellization and then contribute to a decreased CMC value.

Figure 1c shows the  $(\gamma-C)$  plots for  $[\text{C}_{12}\text{mim}]\text{Br}$  and  $[\text{C}_{12}\text{mim}][\text{BF}_4]$  in EAN at 25 °C. Compared with  $[\text{C}_{12}\text{mim}]\text{Br}$ , the CMC and  $\gamma_{\text{CMC}}$  values for  $[\text{C}_{12}\text{mim}][\text{BF}_4]$  are much lower, which is consistent with the observation by Kunz et al.<sup>19</sup> In general, adsorption of the anions onto the micelle surface can reduce the electrostatic repulsion of the head groups, thereby decreasing the CMC values. When replacing  $\text{Br}^-$  with  $[\text{BF}_4]^-$ , the latter can interact with the  $[\text{C}_{12}\text{mim}]^+$  cation more tightly due to its higher basicity, which causes more effective screening of the electrostatic repulsion among the head groups.<sup>9</sup> Meanwhile, this reduced electrostatic repulsion among the hydrophilic groups would cause the molecules to pack more compactly at the air-liquid interface.

The maximum excess surface concentration ( $\Gamma_{\text{max}}$ ) and the area occupied by a single amphiphile molecule at the air-liquid interface ( $A_{\text{min}}$ ), obtained from the Gibbs adsorption isotherm can reflect the molecule arrangement of surfactants at the air-liquid interface.<sup>35</sup> A greater value of  $\Gamma_{\text{max}}$  or a smaller value of  $A_{\text{min}}$  means a denser arrangement of surfactant molecules at the surface of the solution. The obtained  $\Gamma_{\text{max}}$  and  $A_{\text{min}}$  values are listed in Table 1. It is clearly seen that the  $\Gamma_{\text{max}}$  value for  $[\text{C}_{12}\text{mim}][\text{BF}_4]$  is much lower than  $[\text{C}_{12}\text{mim}]\text{Br}$ , indicating a denser arrangement of  $[\text{C}_{12}\text{mim}][\text{BF}_4]$  molecules at the air-liquid interface compared with that of  $[\text{C}_{12}\text{mim}]\text{Br}$ . The result is in agreement with the deduction above. It is also interesting to find that the  $\Gamma_{\text{max}}$  value for  $[\text{C}_{12}\text{pim}]\text{Br}$  is much lower than that for  $[\text{C}_{12}\text{mim}]\text{Br}$ , although  $[\text{C}_{12}\text{pim}]\text{Br}$  possess a much larger headgroup. This result can be justified by the more dispersed charge of the  $[\text{C}_{12}\text{pim}]^+$  cation, which could weaken



the electrostatic repulsion among head groups. In addition, the incorporation of 2,4,6-trimethylphenyl group could produce  $\pi$ - $\pi$  interactions among the adjacent  $[C_{12}mim]Br$  molecules. This  $\pi$ - $\pi$  interaction could attract the molecules to pack more compactly at the air-liquid interface monolayer.<sup>36,37</sup>

**3.2.  $^1H$  NMR Spectra.** It is known from previous  $^1H$  NMR results that in the aqueous solution, imidazolium ILs form intermolecular hydrogen bonding with water, and there is a competition for the hydrogen bonding with the aromatic hydrogens of the cation for the solvent molecules and the counterions.<sup>9,10</sup>  $^1H$  NMR spectra of the surface active imidazolium ILs in EAN at a range of concentrations below and above the CMC are measured to investigate whether the interactions occur when micelles are formed in EAN. The chemical shifts ( $\delta_{obs}$ ) for the protons of the ILs with different structures are presented in Tables 2 and 3. Pronounced changes in the chemical shift of the protons of the alkyl chain and the aromatic ring are observed when structures are varied. The variation of the chemical shift,  $\Delta\delta (= \delta_{obs} - \delta_{mon})$ , for the protons of the surface active ILs and EAN are shown in Figures 3 and 4, respectively.

(a).  *$^1H$  NMR Spectra of Aromatic Ring Protons.* Protons at C-2 of the imidazolium ring are acidic due to the vicinity of electronegative nitrogen and are available for hydrogen bonding with solvent molecules.<sup>32</sup> Typically, the formation of hydrogen bonding from basic solvents to acidic hydrogen atoms moves the chemical shifts of these hydrogen atoms downfield.<sup>38</sup> For  $[C_{12}mim]Br$ , as shown in Figure 3c, a significant downfield shift is observed for the protons at C-2 of the imidazolium ring ( $H_2$ ) upon micellization. Correspondingly,  $H_3$  at the  $[CH_3CH_2NH_3]^+$  cation of EAN shifts upfield (Figure 4c). Similar phenomenon is also observed for  $[C_8mim]Br$  and  $[C_{10}mim]Br$ . This result can

be justified by considering the effect of the formation of hydrogen bonding between the protons at C-2 of the aromatic ring of  $[C_nmim]Br$  and the  $[NO_3]^-$  anion of EAN. When micelles are formed in EAN, protons at C-2 of the imidazolium ring form hydrogen bonding with  $[NO_3]^-$  and the hydrogen bonding between  $[CH_3CH_2NH_3]^+$  and  $[NO_3]^-$  is correspondingly broken. For the purpose of comparison, the  $^1H$  NMR spectra for  $[C_{12}bmim]Br$ , in which H on C-2 is replaced by  $CH_3$ , have been determined. Figure 3d shows the variation of chemical shift for various protons of  $[C_{12}bmim]Br$  as a function of the  $[C_{12}bmim]Br$  concentration. As expected, protons at the methyl group on C-2 shift upfield, contrary to the case for  $[C_{12}mim]Br$ . Meanwhile, the chemical shifts for  $H_a$  at the  $[CH_3CH_2NH_3]^+$  cation are hardly changed, indicating that hydrogen bonding between the cations and anions of EAN keeps intact. This result further indicates that hydrogen bonding is formed between protons at C-2 of the imidazolium ring of  $[C_nmim]Br$  and  $[NO_3]^-$ . It is mentioned that protons at C-4 ( $H_4$ ) and C-5 ( $H_5$ ) of the imidazolium ring for  $[C_8mim]Br$  show behavior different from that of protons at C-2. The upfield shifts for  $H_4$  and  $H_5$  signify that their hydrogen bonding abilities are much lower than  $H_2$ . Therefore, the chemical shifts for  $H_4$  and  $H_5$  are less sensitive to the solvation effect compared with  $H_2$ . The upfield shift behavior of these protons may be due to the ring stacking through  $\pi$ - $\pi$  interactions.<sup>38</sup> The diamagnetic anisotropy of the  $\pi$ - $\pi$  conjugated system formed by the imidazolium ring would bring a remarkable shielding effect and thus lead to an upfield shift of the attached protons.<sup>39</sup> On the basis of theoretical calculations, Palomar<sup>40</sup> also believes that the chemical shift of the protons at the aromatic ring shifts downfield due to the specific interactions with water molecules,

**Table 2. Chemical Shifts  $\delta_{obs}$  (ppm) for Various Protons of  $[C_nmim]Br$  ( $n = 8, 10, 12$ ) in EAN as a Function of Concentration**

C (M)	$\delta_{obs}$						
	$[C_8mim]Br$						
	C-2	C-4	C-5	C-6	C-7	C-8	C-10
0.320	9.2332			4.1689	4.4638	2.0707	1.0366
0.641	9.2500	7.8613	7.7827	4.1485	4.4383	2.0457	1.0040
0.855	9.2557	7.8551	7.7785	4.1316	4.4318	2.0266	0.9844
1.389	9.2578	7.8276	7.7550	4.0788	4.3824	1.9646	0.9111
2.137	9.2811	7.8093	7.7417	4.0209	4.3289	1.8930	0.7883
3.206	9.384	7.7443	7.6967	3.9575	4.2714	1.7970	0.7072

C (M)	$\delta_{obs}$				
	$[C_{10}mim]Br$				
	C-2	C-6	C-7	C-8	C-10
0.153	9.2336	4.1882	4.4831	2.0961	1.0688
0.306	9.2424	4.1806	4.4775	2.0873	1.0662
0.408	9.2434	4.1646	4.4635	2.0714	1.0579
0.663	9.2564	4.1535	4.4565	2.0602	1.0323
1.020	9.2754	4.1257	4.4324	2.0308	0.9991
1.530	9.3071	4.0982	4.4088	2.0011	0.9632

C (M)	$\delta_{obs}$				
	$[C_{12}mim]Br$				
	C-2	C-6	C-7	C-8	C-10
0.0474	9.218	4.1764	4.4712	2.0853	1.0711
0.0948	9.2201	4.1755	4.4693	2.0846	1.0702
0.1264	9.2254	4.1739	4.4689	2.0842	1.0699
0.2050	9.2386	4.1705	4.4677	2.0818	1.0612
0.3160	9.2529	4.1566	4.4610	2.0708	1.0477
0.4740	9.2761	4.1347	4.4494	2.0516	1.0225

**Table 3.** Chemical Shifts  $\delta_{\text{obs}}$  (ppm) for Various Protons of  $[\text{C}_{12}\text{bmim}]\text{Br}$ ,  $[\text{C}_{12}\text{pim}]\text{Br}$ , and  $[\text{C}_{12}\text{mim}][\text{BF}_4]$  in EAN as a Function of Concentration

C (M)	$\delta_{\text{obs}}$				
	$[\text{C}_{12}\text{bmim}]\text{Br}$				
	C-2	C-6	C-7	C-8	C-10
0.0336	2.9425	4.1114	4.4416	2.0776	1.1357
0.0672	2.9360	4.1048	4.4361	2.0717	1.1292
0.0896	2.9355	4.1053	4.4368	2.0716	1.1301
0.1456	2.9298	4.1007	4.4339	2.0683	1.1257
0.2800	2.9156	4.0879	4.4259	2.0581	1.1146
0.3360	2.9018	4.0771	4.4159	2.0474	1.1091

C (M)	$\delta_{\text{obs}}$							
	$[\text{C}_{12}\text{pim}]\text{Br}$							
	C-2	C-5	C-6,7	C-8,9	C-10	C-11	C-12	C-14
0.0153	9.6199	8.2586	2.3458	7.3815	2.6175	4.6710	2.2667	1.1268
0.0306	9.6116	8.2559	2.3357	7.3717	2.6074	4.6650	2.2605	1.1246
0.0408	9.6218	8.2575	2.3395	7.3708	2.6098	4.6660	2.2619	1.1233
0.0663	9.6153	8.2497	2.3318	7.3669	2.6025	4.6542	2.2527	1.1128
0.1020	9.6308	8.2495	2.3144	7.3440	2.5802	4.6376	2.2367	1.1044
0.1530	9.6389	8.2488	2.3033	7.3308	2.5670	4.6280	2.2256	1.0985

C (M)	$\delta_{\text{obs}}$				
	$[\text{C}_{12}\text{mim}][\text{BF}_4]$				
	C-2	C-6	C-7	C-8	C-10
0.0321	9.2147	4.1801	4.4741	2.0894	1.0757
0.0642	9.2217	4.1818	4.4774	2.0922	1.0779
0.0856	9.2257	4.1820	4.4787	2.0934	1.0784
0.1391	9.2243	4.1704	4.4703	2.0837	1.0685
0.2140	9.2254	4.1622	4.4666	2.0795	1.0623
0.3210	9.2209	4.1454	4.4541	2.0679	1.0538

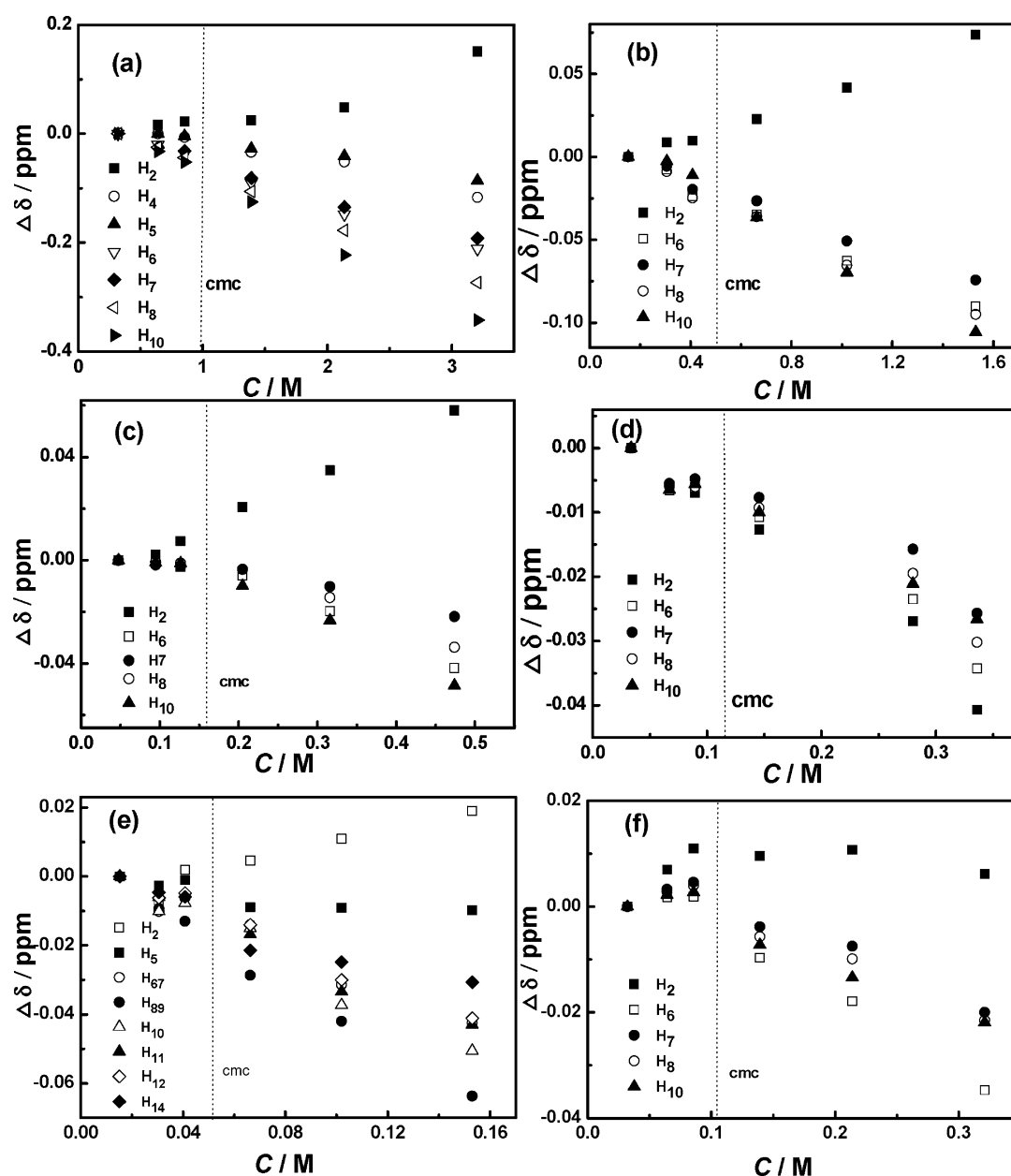
while the nonspecific polarization effects of the solvent cage provide the opposite effect.

Figure 3f shows the variation of chemical shift for protons of  $[\text{C}_{12}\text{mim}][\text{BF}_4]$  as a function of concentration. The protons at C-2 of the imidazolium ring of  $[\text{C}_{12}\text{mim}][\text{BF}_4]$  also show a downfield shift but with a much lower magnitude than that of  $[\text{C}_{12}\text{mim}]\text{Br}$ . This change in chemical shift indicates that there is a competition for the interaction of aromatic protons with the solvent and the counterions in the EAN system. It has been proved above that for  $[\text{C}_{12}\text{mim}]\text{Br}$ ,  $[\text{C}_{12}\text{mim}]^+$  can interact with  $[\text{NO}_3]^-$  through electrostatic and hydrogen bonding interactions. When  $\text{Br}^-$  is replaced by  $[\text{BF}_4]^-$ , the interaction between the aromatic hydrogen atoms, primarily  $\text{H}_2$ , and  $[\text{BF}_4]^-$  becomes stronger due to the higher basicity of  $[\text{BF}_4]^-$ . This more intimate interaction reduces the possibility of the interaction between  $[\text{C}_{12}\text{mim}]^+$  and  $[\text{NO}_3]^-$ . Therefore, the chemical shift for  $\text{H}_2$  of  $[\text{C}_{12}\text{mim}][\text{BF}_4]$  is less sensitive to solvation effect than  $[\text{C}_{12}\text{mim}]\text{Br}$ .<sup>8,9</sup>

The change in chemical shift on micelle formation,  $\delta_{\text{diff}}$  ( $=\delta_{\text{mic}} - \delta_{\text{mon}}$ ), can reflect the change in chemical environment.<sup>41</sup> It is known that the chemical shifts upon micellization are mainly affected by the combination of the “medium effect”, caused by the movement of surfactant molecules from the solvent to micelle, and the “conformation effect”, resulting from a partial changeover from gauche to trans conformation in the alkyl chains upon micellization.<sup>42,43</sup> Typically, a positive value of  $\delta_{\text{diff}}$  is observed under the influence of the “medium effect” and the “conformation effect”.<sup>44</sup> Figure 5 shows the comparison of the  $\delta_{\text{diff}}$  values for  $\text{H}_2$  among the ILs with different structures. Except for  $[\text{C}_{12}\text{bmim}]\text{Br}$ , the  $\delta_{\text{diff}}$  values for  $\text{H}_2$  for

other ILs are all positive due to the so-called “medium effect”. The  $\delta_{\text{diff}}$  values varies in the order:  $[\text{C}_8\text{mim}]\text{Br} > [\text{C}_{10}\text{mim}]\text{Br} > [\text{C}_{12}\text{mim}]\text{Br} > [\text{C}_{12}\text{pim}]\text{Br} > [\text{C}_{12}\text{mim}][\text{BF}_4]$ . It is clear that the  $\delta_{\text{diff}}$  values decrease with the increase of alkyl chain length in position C-1. This result signifies that the solvation effect for  $\text{H}_2$  decreases with the increase of alkyl chain length. In addition, the  $\delta_{\text{diff}}$  value also decreases as an extra aromatic group, the 2, 4, 6-trimethylphenyl group, is incorporated in position C-3. The reduced solvation effect for  $\text{H}_2$  caused by the increased solvophobicity of the headgroup may be responsible for this behavior. The observation above is in agreement with the case in water, where the interaction between water and the aromatic hydrogens for imidazolium ILs decreases when the side-chains in positions C-1 and C-3 become more hydrophobic.<sup>9</sup> The much lower  $\delta_{\text{diff}}$  value for  $[\text{C}_{12}\text{mim}][\text{BF}_4]$  is concordant with the fact discussed above, that is,  $\text{H}_2$  for  $[\text{C}_{12}\text{mim}][\text{BF}_4]$  is less sensitive to solvation effect than that of  $[\text{C}_{12}\text{mim}]\text{Br}$ . From the results above, it is obvious that the interactions between the aromatic hydrogens and EAN vary as a function of the nature of the counterions and the solvophobicity of the side-chain bonded to the imidazolium cation.

(b). <sup>1</sup>H NMR Spectra of Alkyl Chain Protons. As can be seen from Figure 3, protons of the alkyl chain for all the ILs show an upfield shift on aggregation. The upfield shift for the protons of the alkyl chain may be attributed to the average effect of conformational changes and aromatic ring current effect-induced shielding effect.<sup>10,39,44</sup> Since an upfield shift can be related to an increasing importance of the gauche conformation, the micelle formation may be accompanied by a partial changeover from trans to gauche conformations in the alkyl chain.<sup>10</sup> The aromatic



**Figure 3.** Variation of chemical shifts for various protons of surface active ILs at different concentrations at 25 °C; (a)  $[C_8\text{mim}]\text{Br}$ , (b)  $[C_{10}\text{mim}]\text{Br}$ , (c)  $[C_{12}\text{mim}]\text{Br}$ , (d)  $[C_{12}\text{bmim}]\text{Br}$ , (e)  $[C_{12}\text{pim}]\text{Br}$ , and (f)  $[C_{12}\text{mim}][\text{BF}_4]$ .

ring-induced shielding effect can also lead to an upfield shift.<sup>39,44</sup> The  $\delta_{\text{diff}}$  values for the protons of the alkyl chain for different ILs are calculated and shown in Figure 6. For  $[C_n\text{mim}]\text{Br}$ , the  $\delta_{\text{diff}}$  values for all the protons of the alkyl chain are negative and the absolute value for the protons of the methyl group attached directly to the aromatic ring ( $H_7$ ) is smaller than those for other protons of the alkyl chain ( $H_8$ ,  $H_{10}$ ). This result is possibly due to the lesser shielding of the protons of  $H_7$  by the aromatic ring. It is mentioned that the  $\delta_{\text{diff}}$  values for  $[C_{12}\text{mim}][\text{BF}_4]$  are almost the same as  $[C_{12}\text{mim}]\text{Br}$ , indicating that the chemical shifts for the protons of the alkyl chain is independent of the nature of counterions.

When the 2,4,6-trimethylphenyl group is incorporated into the headgroup, the  $\delta_{\text{diff}}$  value for protons of the methyl group attached directly to the aromatic ring ( $H_{11}$ ) is still negative but its absolute value becomes larger than the other protons of the

alkyl chain ( $H_{12}$ ,  $H_{14}$ ). This result is probably caused by some shielding by the benzene ring of the 2,4,6-trimethylphenyl group. It is known that protons located above and below the plane of aromatic ring resonate at a higher field due to the shielding effect.<sup>45</sup> Thus, the 2,4,6-trimethylphenyl group may bend into the solvophobic moieties slightly and lies parallel to the interface, which may cause the protons near the headgroup to move into the field of the ring current and then shift to the upfield.<sup>44</sup> Similar result has been observed for the micelle formation of  $[C_{12}\text{pim}]\text{Br}$  in aqueous solution.<sup>36</sup>

Since the solvent effects are small for alkyl groups, the change in the chemical shift of the protons of the terminal methyl group in the alkyl chain as a function of concentration can be used to determine the aggregation concentration.<sup>46</sup> Based on the fast exchange of the surfactant molecules in the NMR time scale, the observed chemical

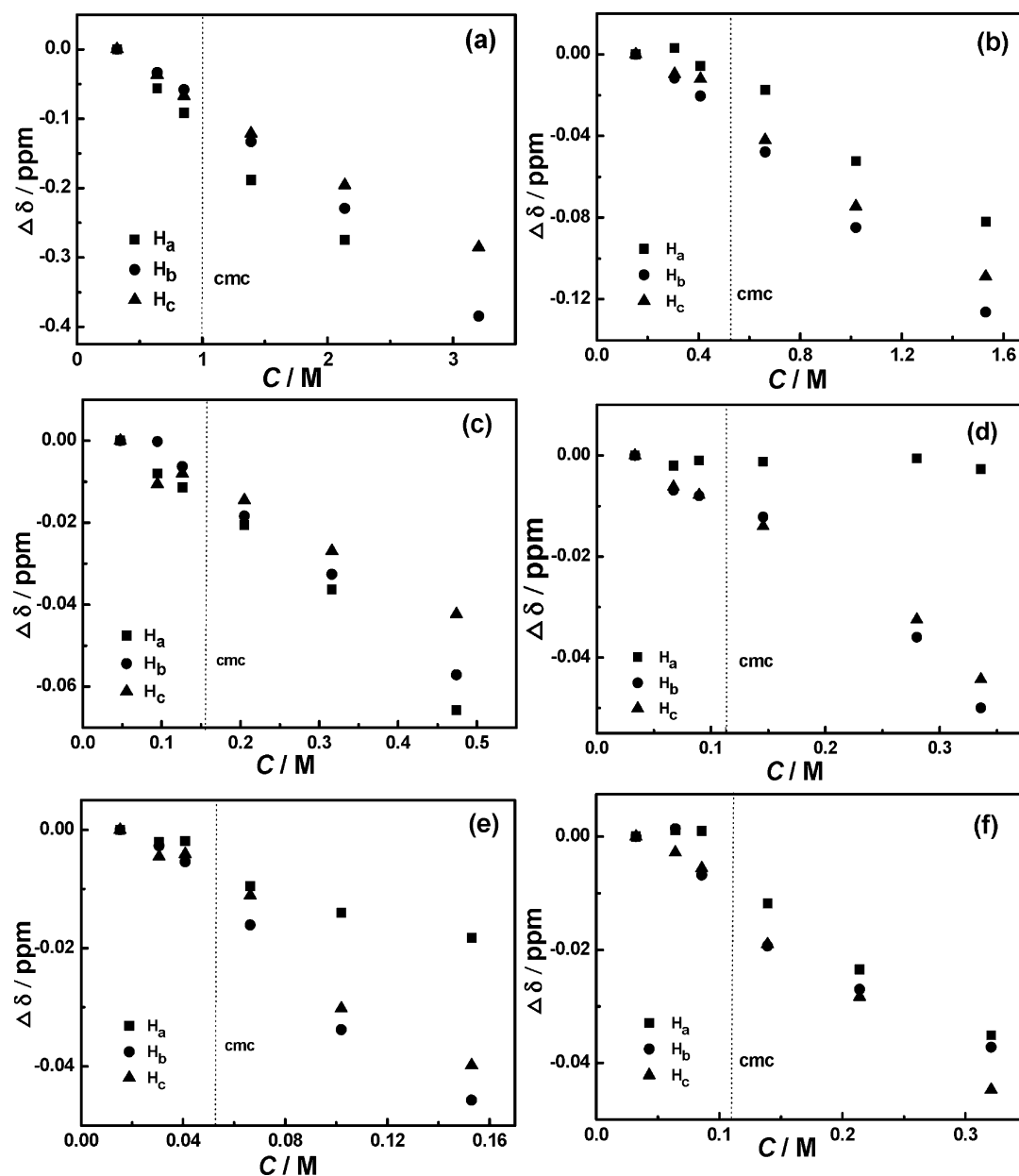


**Figure 4.** Variation of chemical shifts for various protons of EAN at different concentrations at 25 °C; (a)  $[C_8mim]Br$ , (b)  $[C_{10}mim]Br$ , (c)  $[C_{12}mim]Br$ , (d)  $[C_{12}bmim]Br$ , (e)  $[C_{12}pim]Br$ , and (f)  $[C_{12}mim][BF_4]$ .

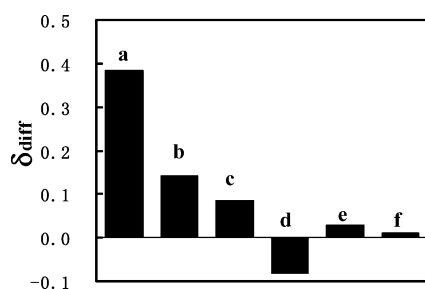


**Figure 5.** Comparison of  $\delta_{diff}$  ( $\delta_{mic} - \delta_{mon}$ ) for the protons at C-2 of imidazolium ring among the ILs with different structures. (a)  $[C_8mim]Br$ , (b)  $[C_{10}mim]Br$ , (c)  $[C_{12}mim]Br$ , (d)  $[C_{12}bmim]Br$ , (e)  $[C_{12}pim]Br$ , and (f)  $[C_{12}mim][BF_4]$ .

shift ( $\delta_{obs}$ ) can be expressed as a weighted average of the chemical shifts of the monomer ( $\delta_{mon}$ ) and the micelle ( $\delta_{mic}$ ).

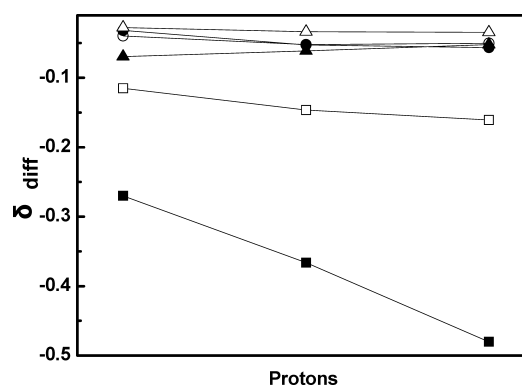


**Figure 6.** Plots of  $\delta_{diff}$  ( $\delta_{mic} - \delta_{mon}$ ) for the protons of the alkyl chain for various ILs. (■)  $[C_8mim]Br$  ( $H_7$ ,  $H_8$ ,  $H_{10}$ ), (□)  $[C_{10}mim]Br$  ( $H_7$ ,  $H_8$ ,  $H_{10}$ ), (●)  $[C_{12}mim]Br$  ( $H_7$ ,  $H_8$ ,  $H_{10}$ ), (○)  $[C_{12}bmim]Br$  ( $H_7$ ,  $H_8$ ,  $H_{10}$ ), (▲)  $[C_{12}pim]Br$  ( $H_{11}$ ,  $H_{12}$ ,  $H_{14}$ ), and (Δ)  $[C_{12}mim][BF_4]$  ( $H_7$ ,  $H_8$ ,  $H_{10}$ ).



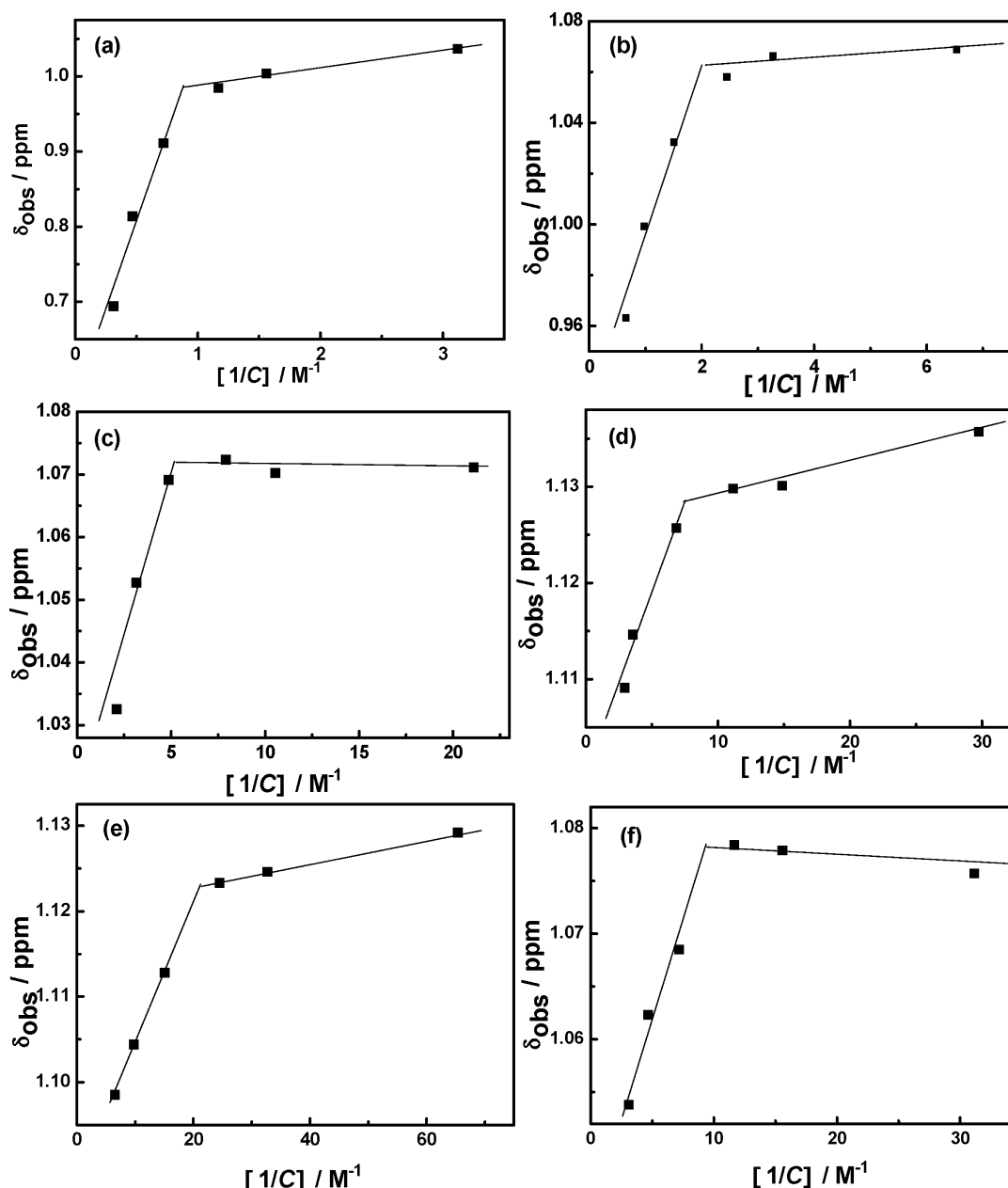


**Figure 7.** Variation of  $\delta_{\text{obs}}$  for the protons of the terminal carbon of alkyl chain against the reciprocal concentration of  $[\text{C}_8\text{mim}]\text{Br}$  (a),  $[\text{C}_{10}\text{mim}]\text{Br}$  (b),  $[\text{C}_{12}\text{mim}]\text{Br}$  (c),  $[\text{C}_{12}\text{bmim}]\text{Br}$  (d),  $[\text{C}_{12}\text{pim}]\text{Br}$  (e), and  $[\text{C}_{12}\text{mim}][\text{BF}_4]$  (f).

$$\delta_{\text{obs}} = \delta_{\text{mon}} \left( \frac{C_{\text{mon}}}{C_T} \right) + \delta_{\text{mic}} \left( \frac{C_{\text{mic}}}{C_T} \right) \quad (2)$$

where  $C_{\text{mon}}$  and  $C_{\text{mic}}$  are the concentrations of surfactant existing as monomers and micelles, respectively.  $C_T$  is the total concentration of surfactant. It is assumed that the monomer concentration is constant above the CMC, thus

$$\delta_{\text{obs}} = \delta_{\text{mic}} - \left( \frac{\text{cmc}}{C_T} \right) (\delta_{\text{mic}} - \delta_{\text{mon}}) \quad (3)$$

$\delta_{\text{mon}}$  and  $\delta_{\text{mic}}$  can be estimated by extrapolation of the plots of  $\delta_{\text{obs}}$  versus  $C_T$  and  $\delta_{\text{obs}}$  versus  $1/C_T$ , respectively. Figure 7 shows the  $\delta_{\text{obs}}$  values versus  $1/C_T$  plots for the terminal protons of the surface active ILs. At low concentrations,  $\delta_{\text{obs}}$  keeps almost constant and then changes rapidly at higher concentrations. The sudden increase

of slope is a consequence of micelle formation, and the break point corresponds to the CMC (Table 2). It can be seen that the obtained CMC values are in close agreement with those obtained from the surface tension measurements.

#### (c). $^1\text{H}$ NMR Spectra of Ethylammonium Cation Protons.

In EAN, three-dimensional hydrogen bonding network can be formed between the hydrogen atoms in  $[\text{CH}_3\text{CH}_2\text{NH}_3]^+$  cations and the oxygen atoms in  $[\text{NO}_3]^-$  anions.<sup>14</sup> When the surface active ILs are added into EAN, hydrogen bonding interactions can also occur between  $[\text{CH}_3\text{CH}_2\text{NH}_3]^+$  and the anions of surface active ILs, as well as  $[\text{NO}_3]^-$  and the cations of surface active ILs. Thus the information about the involvement of EAN in the micelle formation can also be obtained by analyzing the change in the chemical shift of protons of EAN during micellization. The chemical shifts for protons of the  $[\text{CH}_3\text{CH}_2\text{NH}_3]^+$  cation for different surface active IL at

**Table 4.** Chemical Shifts  $\delta_{\text{obs}}$  (ppm) for Protons in the  $[\text{CH}_3\text{CH}_2\text{NH}_3]^+$  Cation as a Function of Concentration in the EAN Solutions of Different ILs

$[\text{C}_8\text{mim}]\text{Br}$				$[\text{C}_{10}\text{mim}]\text{Br}$			
C (M)	$\delta_{\text{obs}}$			C (M)	$\delta_{\text{obs}}$		
	$\text{H}_a$	$\text{H}_b$	$\text{H}_c$		$\text{H}_a$	$\text{H}_b$	$\text{H}_c$
0.320	7.7950	3.3695	1.5139	0.153	7.8184	3.3951	1.5275
0.641	7.7390	3.3360	1.4770	0.306	7.8216	3.3835	1.5179
0.855	7.7037	3.3113	1.4465	0.408	7.8127	3.3747	1.5155
1.389	7.6068	3.2365	1.3924	0.663	7.7871	3.3473	1.4855
2.137	7.5204	3.1403	1.3183	1.020	7.7662	3.3102	1.4530
3.206		2.9850	1.2287	1.530	7.7323	3.2688	1.4187
$[\text{C}_{12}\text{mim}]\text{Br}$				$[\text{C}_{12}\text{bmim}]\text{Br}$			
C (M)	$\delta_{\text{obs}}$			C (M)	$\delta_{\text{obs}}$		
	$\text{H}_a$	$\text{H}_b$	$\text{H}_c$		$\text{H}_a$	$\text{H}_b$	$\text{H}_c$
0.0474	7.8286	3.3861	1.5259	0.0336	7.8594	3.4492	1.5904
0.0948	7.8206	3.3859	1.5153	0.0672	7.8574	3.4403	1.5822
0.1264	7.8172	3.3798	1.5179	0.0896	7.8588	3.4412	1.5826
0.2050	7.8080	3.3677	1.5114	0.1456	7.8584	3.437	1.5764
0.3160	7.7923	3.3535	1.4990	0.2800	7.8582	3.4132	1.5579
0.4740	7.7628	3.329	1.4836	0.3360	7.8517	3.3992	1.5461
$[\text{C}_{12}\text{pim}]\text{Br}$				$[\text{C}_{12}\text{mim}][\text{BF}_4]$			
C (M)	$\delta_{\text{obs}}$			C (M)	$\delta_{\text{obs}}$		
	$\text{H}_a$	$\text{H}_b$	$\text{H}_c$		$\text{H}_a$	$\text{H}_b$	$\text{H}_c$
0.0153	7.8564	3.4481	1.5864	0.0321	7.8069	3.3905	1.5305
0.0306	7.8543	3.4454	1.5819	0.0642	7.8080	3.3919	1.5227
0.0408	7.8545	3.4427	1.5823	0.0856	7.8079	3.3837	1.5321
0.0663	7.8469	3.4320	1.5753	0.1391	7.7951	3.3712	1.5115
0.1020	7.8424	3.4143	1.5562	0.2140	7.7834	3.3635	1.5022
0.1530	7.8381	3.4024	1.5466	0.3210	7.7718	3.3533	1.4858

different concentrations are listed in Table 4. Figure 4 shows the variation of chemical shift for protons of the  $[\text{CH}_3\text{CH}_2\text{NH}_3]^+$  cation as a function of the surface active IL concentration. It is clear that the chemical shifts for  $\text{H}_a$  moves upfield except for that of  $[\text{C}_{12}\text{bmim}]\text{Br}$ , which keeps almost constant before and after CMC. The upfield shifts for  $\text{H}_a$  may be caused by the consequence that the hydrogen bonding between  $[\text{NO}_3]^-$  and  $[\text{CH}_3\text{CH}_2\text{NH}_3]^+$  is weakened.<sup>38</sup> While in the case of  $[\text{C}_{12}\text{bmim}]\text{Br}$ , in which the proton on C-2 of is replaced with  $\text{CH}_3$ , the hydrogen bonding between  $[\text{NO}_3]^-$  and  $[\text{CH}_3\text{CH}_2\text{NH}_3]^+$  keeps intact. It is interesting that  $\text{H}_b$  and  $\text{H}_c$  also shifts toward higher magnetic field during micellization. This result is mainly caused by the fact that solvophobic interaction exists between the solvophobic portion of the  $[\text{CH}_3\text{CH}_2\text{NH}_3]^+$  cations and the solvophobic parts of the surfactant molecules.<sup>47</sup> In other words, the ethylammonium cations may have the tendency to penetrate into the micelles due to this solvophobic interaction.

#### 4. CONCLUSIONS

In this study, it was observed that the alkyl chain length, the structure of the cations, and the nature of counterions have significant effect on the surface properties and aggregation behavior of surface active imidazolium ILs in EAN. The CMC was detected only when the alkyl chain length is longer than eight and the CMC values decrease with the elongation of the hydrocarbon chain. Both the C-2 methylation and incorporation of the aromatic group increase the solvophobicity of head groups and then contribute to lower CMC values. The CMC and  $A_{\text{min}}$  values are also decreased when replacing  $\text{Br}^-$

with  $[\text{BF}_4]^-$ . The increased basicity of counterions causes more intimate interactions between cations and counterions, and thus leads to more effective screening of the electrostatic repulsion among the cations.  $^1\text{H}$  NMR results show that protons at C-2 on the imidazolium ring form hydrogen bonding with  $[\text{NO}_3]^-$ , and thus the hydrogen bonding between  $[\text{CH}_3\text{CH}_2\text{NH}_3]^+$  and  $[\text{NO}_3]^-$  is weakened. It was also found that the interactions between the aromatic hydrogens and EAN become weaker with the increase of the basicity of counterions and the hydrophobicity of the side-chains bonded to the imidazolium cation. The chemical shifts for the protons of the alkyl chain depend on the average effect of conformational changes and aromatic ring current effect-induced shielding effect, but is independent of the nature of counterions. And the conformation of the alkyl chain may be changed partially from trans to gauche conformations during micelle formation. Solvophobic effect may exist between the solvophobic portion of the EAN molecules and the hydrophobic parts of the surfactant molecules.

#### AUTHOR INFORMATION

##### Corresponding Author

\*E-mail: lqzheng@sdu.edu.cn. Phone: +86-531-88366062. Fax: +86-531-88564750.

##### Notes

The authors declare no competing financial interest.

#### ACKNOWLEDGMENTS

The authors are grateful to the National Natural Science Foundation of China (No. 50972080 and 91127017) and the

National Basic Research Program (2009CB930101) for financial support.

## REFERENCES

- (1) Rogers, R. D.; Seddon, K. R. *Science* **2003**, *302*, 792–793.
- (2) Welton, T. *Chem. Rev.* **1999**, *99*, 2071–2084.
- (3) Bowers, J.; Butts, P.; Martin, J.; Vergara-Gutierrez, C.; Heenan, K. *Langmuir* **2004**, *20*, 2191–2198.
- (4) Goodchild, I.; Collier, L.; Millar, S. L.; Prokès, I.; Lord, J. C. D.; Butts, C. P. B.; Bowers, J.; Webster, J. R. P.; Heenan, R. K. *J. Colloid Interface Sci.* **2007**, *307*, 445–468.
- (5) Blesic, M.; Marques, M. H.; Plechkova, N. V.; Seddon, K. R.; Rebelo, L. P. N.; Lopes, A. *Green Chem.* **2007**, *9*, 481–490.
- (6) Blesic, M.; Lopes, A.; Melo, E.; Petrovski, Z.; Plechkova, N. V.; Canongia Lopes, J. N.; Seddon, K. R.; Rebelo, L. P. N. *J. Phys. Chem. B* **2008**, *112*, 8645–8650.
- (7) Wang, H. Y.; Wang, J. J.; Zhang, S. B.; Xuan, X. P. *J. Phys. Chem. B* **2008**, *112*, 16682–16689.
- (8) Headley, A. D.; Jackson, N. M. *J. Phys. Org. Chem.* **2002**, *15*, 52–55.
- (9) Headley, A. D.; Kotti, S. R. S. S.; Nam, J.; Li, K. J. *J. Phys. Org. Chem.* **2005**, *18*, 1018–1022.
- (10) Singh, T.; Kumar, A. *J. Phys. Chem. B* **2007**, *111*, 7843–7851.
- (11) Wang, J. J.; Wang, H. Y.; Zhang, S. L.; Zhang, H. C.; Zhao, Y. *J. Phys. Chem. B* **2007**, *111*, 6181–6188.
- (12) Modarelli, A.; Sifaoui, H.; Mielcarz, M.; Domńska, U.; Rogalski, M. *Colloids Surf., A* **2007**, *302*, 181–185.
- (13) Greaves, T. L.; Drummond, C. J. *Chem. Soc. Rev.* **2008**, *37*, 1709–1726.
- (14) Greaves, T. L.; Drummond, C. J. *Chem. Rev.* **2008**, *108*, 206–237.
- (15) Evans, D. F.; Yamauchi, A.; Roman, R.; Casassa, E. Z. *J. Colloid Interface Sci.* **1982**, *88*, 89–96.
- (16) Evans, D. F.; Yamauchi, A.; Wei, G. J.; Bloomfield, V. A. *J. Phys. Chem.* **1983**, *87*, 3537–3541.
- (17) Velasco, S. B.; Turmine, M.; Di Caprio, D.; Letellier, P. *Colloids Surf., A* **2006**, *275*, 50–54.
- (18) Araos, M. U.; Warr, G. G. *Langmuir* **2008**, *24*, 9354–9360.
- (19) Thomaier, S.; Kunz, W. *J. Mol. Liq.* **2007**, *130*, 104–107.
- (20) Kang, W. P.; Dong, B.; Gao, Y. A.; Zheng, L. Q. *Colloid Polym. Sci.* **2010**, *288*, 1225–1232.
- (21) Li, N.; Zhang, S. H.; Zheng, L. Q.; Dong, B.; Li, X. W.; Yu, L. *J. Phys. Chem. Chem. Phys.* **2008**, *10*, 1–3.
- (22) Obliosca, J. M.; Arco, S. D.; Huang, M. H. *J. Fluoresc.* **2007**, *17*, 613–618.
- (23) Dupont, J.; Consorti, C. S.; Suarez, P. A. Z.; de Souza, R. F.; Fulmer, S. L.; Richardson, D. P.; Smith, T. E.; Wolff, S. *Org. Synth.* **2002**, *79*, 236–241.
- (24) Ahrens, S.; Peritz, A.; Strassner, T. *Angew. Chem., Int. Ed.* **2009**, *48*, 7908–7910.
- (25) Fox, D. M.; Awad, W. H.; Gilman, J. W.; Maupin, P. H.; DeLongd, H. C.; Truloved, P. C. *Green Chem.* **2003**, *5*, 724–727.
- (26) Holbrey, J. D.; Seddon, K. R. *J. Chem. Soc., Dalton Trans. Inorg. Chem.* **1999**, *13*, 2133–2139.
- (27) Evans, D. F.; Chen, S. H.; Schriver, G. W.; Arnett, E. M. *J. Am. Chem. Soc.* **1981**, *103*, 481–482.
- (28) Dong, B.; Li, N.; Zheng, L. Q.; Yu, L.; Inoue, T. *Langmuir* **2007**, *23*, 4178–4182.
- (29) Dong, B.; Zhao, X. Y.; Zheng, L. Q.; Zhang, J.; Li, N.; Inoue, T. *Colloids Surf., A* **2008**, *317*, 666–672.
- (30) Shinoda, K. *Colloidal Surfactant*; Academic Press: New York, 1963; Chapter 1.
- (31) Zhao, G. X.; Zhu, B. Y. *Principles of Surfactant Action*; China Light Industry Press: Beijing, 2003.
- (32) Arduengo, A. J. P.; Harlow, R. L.; Kline, M. J. *Am. Chem. Soc.* **1991**, *113*, 361.
- (33) Kato, H.; Miki, K.; Mukai, T.; Nishikawa, K. *J. Phys. Chem. B* **2009**, *113*, 14754–14760.
- (34) Fan, Y. R.; Li, Y. J.; Yuan, G. C.; Wang, Y. L.; Wang, J. B.; Han, C. C.; Yan, H. K.; Li, Z. X.; Thomas, R. K. *Langmuir* **2005**, *21*, 3814–3820.
- (35) Jaycock, M. J.; Parfitt, G. D. *Chemistry of Interfaces*; John Wiley and Sons: New York, 1981.
- (36) Shi, L. J.; Li, N.; Yan, H.; Gao, Y. A.; Zheng, L. Q. *Langmuir* **2011**, *27*, 1618.
- (37) Li, Y. J.; Reeve, J.; Wang, Y. L.; Thomas, R. K.; Wang, J. B.; Yan, H. K. *J. Phys. Chem. B* **2005**, *109*, 16070–16074.
- (38) Bonhôte, P.; Dias, A. P.; Papageorgiou, N.; Kalyanasundaram, K.; Grätzel, M. *Inorg. Chem.* **1996**, *35*, 1168–1178.
- (39) Dong, B.; Gao, Y. A.; Su, Y. J.; Zheng, L. Q.; Xu, J. K.; Inoue, T. *J. Phys. Chem. B* **2010**, *114*, 340–348.
- (40) Palomar, J.; Ferro, V. R.; Gilarranz, M. A.; Rodriguez, J. J. *J. Phys. Chem. B* **2007**, *111*, 168–180.
- (41) Davey, T. W.; Ducker, W. A.; Hayman, A. R. *Langmuir* **2000**, *16*, 2430–2435.
- (42) Huang, X.; Han, Y. C.; Wang, Y. X.; Wang, Y. L. *J. Phys. Chem. B* **2007**, *111*, 12439–12446.
- (43) Persson, B. O.; Drakenberg, T.; Lindman, B. *J. Phys. Chem.* **1976**, *80*, 2124–2125.
- (44) Okano, L. T.; El Seoud, O. A.; Halstead, T. K. *Colloid Polym. Sci.* **1997**, *275*, 138–145.
- (45) Shimizu, S.; El Seoud, O. A. *Langmuir* **2003**, *19*, 238–243.
- (46) Goon, P.; Das, S.; Clemett, C. J.; Tiddy, T.; Kumar, V. V. *Langmuir* **1997**, *13*, 5577–5582.
- (47) Li, N.; Zhang, S. H.; Zheng, L. Q.; Wu, J. P.; Li, X. W.; Yu, L. *J. Phys. Chem. B* **2008**, *112*, 12453–12460.